Searches for New Physics at the Tevatron in Photon and Jet Final States

Shin-Shan Eiko Yu
Fermi National Accelerator Laboratory
Batavia, IL 60510, U.S.A.
for the CDF and DØ Collaborations

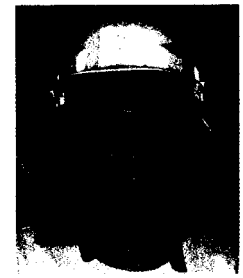

We present the results of searches for non-standard model phenomena in photon and jet final states. These searches use data from integrated luminosities of 0.7–2.7 fb^{-1} of $p\bar{p}$ collisions at $\sqrt{s} = 1.96$ TeV, collected with the CDF and DØ detectors at the Fermilab Tevatron. No significant excess in data has been observed. We report limits on the parameters of several models, including: large extra dimension, compositeness, leptoquarks, and supersymmetry.

1 Introduction

To date, almost all experimental results have agreed with the predictions by the standard model (SM) of particle physics. However, several limitations indicate that the SM is not the final theory, for example: (i) Gravity is not yet described by the SM. (ii) The electroweak symmetry is broken at energy ≈ 1 TeV, much smaller than the Planck scale $M_{Pl} \approx 10^{16}$ TeV (hierarchy problem). (iii) The SM does not provide candidates for the dark matter or dark energy. In this document, we present the results of searches inspired by extensions of the SM: large extra dimension [1], compositeness [2], leptoquarks [3], and supersymmetry (SUSY) [4,5,6]. Specifically, we focus on the searches in final states that contain photons (γ), jets (j), or b-jets (b). These searches are based on 0.7 2.7 fb^{-1} of $p\bar{p}$ collisions at $\sqrt{s} = 1.96$ TeV, recorded with the CDF and DØ detectors at the Fermilab Tevatron. Sections 2–5 describe the basic ideas of the analysis techniques and present the results of these searches. Section 6 gives the conclusion.

2 Searches for Large Extra Spatial Dimensions

In the large extra spatial dimensions model (LED)[1], SM particles are confined to a 4-dimensional membrane and graviton propagates in the 4+n_d dimension, where n_d stands for the number of

additional compactified spatial dimensions. The observed Planck scale M_{pl}, the fundamental Planck scale M_D, and the size of the extra dimensions R are related by the Gauss Law: $[M_{pl}]^2 = 8\pi R^{n_d}[M_D]^{n_d+2}$. If R is large compared to the Planck length $\approx 1.6 \times 10^{-33}$ cm, M_D can be as low as 1 TeV and effectively solves the hierarchy problem. The graviton appears to us, who live in the 4 dimension, like series of Kaluza-Klein (KK) states with meV to MeV of mass splittings that can be integrated into a massive KK graviton (G_{KK}). In hadron colliders, we can use two methods to search for indications of LED:

1. Look for deviations of the production cross-sections from the SM either in absolute values or in shapes, due to exchange of the virtual graviton that travels through the extra dimensions. The interference and direct gravity terms in the LED cross section are parameterized by $\mathcal{F}/M_S^4$, where M_S is the ultraviolet cutoff of the sum over KK states. or the so-called effective Planck scale. The formalisms of $\mathcal{F}$ include: (i) $\mathcal{F} = 1$ (GRW)[7], (ii) $\mathcal{F} = \ln(M_S^2/\hat{s})$ for $n_d = 2$ and $\mathcal{F} = 2/(n_d - 2)$ for $n_d > 2$, where $\hat{s}$ is the center-of-mass energy of the partonic subprocess (HLZ)[8], and (iii) $\mathcal{F} = \pm 2/\pi$ (Hewett)[9]. Sections 2.1 and 2.2 describe this type of LED search using the invariant mass and angular distributions of di-electromagnetic (di-EM) and dijet channels, respectively.

2. Look for emission of real G_{KK} through the production channels $q\bar{q} \to gG_{KK}$, $qg \to qG_{KK}$, and $q\bar{q} \to \gamma G_{KK}$, with signatures of mono-jet or mono-photon and large $\not\!\!E_T$. Section 2.3 describes this type of LED search using the $\gamma \not\!\!E_T$ final state.

2.1 Search for LED in the Dielectron and Diphoton Channels

The DØ Collaboration has looked for LED in 1.1 fb^{-1} of $p\bar{p}$ collisions, using the two-dimensional distributions of invariant mass $M_{ee,\gamma\gamma}$ and angular variable $|\cos\theta^*|$ [a] of two EM objects (combining dielectron and diphoton channels) [10]. The two EM objects must have $E_T > 25$ GeV each,[b] and are reconstructed either both in the central EM calorimeter ($|\eta| \; o \; 1.1$) or one in the central and one in the forward EM calorimeters ($1.5 \; o \; |\eta| \; o \; 2.4$). For the background from SM Drell-Yan and diphoton production, the shapes and absolute normalizations of their distributions are modeled with the PYTHIA event generator[11], followed by a DØ detector full simulation and a mass-dependent k-factor (~ 1.34) for the next-to-leading order effect. For the QCD background from γ+jet and multi-jet events, the shapes of their spectra are modeled using the data with at least one EM object that fails the requirement on the shower profile. The normalization of the QCD background is obtained by fitting $M_{ee,\gamma\gamma}$ in the range of 60–140 GeV/c^2, where we expect no LED signal, to a linear combination of the SM $ee/\gamma\gamma$ production and QCD background. Then, the fit result is extrapolated to the mass region above 140 GeV/c^2. Figure 1 shows the $M_{ee,\gamma\gamma}$ and $|\cos\theta^*|$ distributions. Without observing discrepancy from the background prediction, lower limits on M_S are obtained at the 95% confidence level (C.L.): 1.62 TeV using the GRW formalism, and 2.09–1.29 TeV using the HLZ formalism for $n_d = 2 - 7$. These are currently the best limits on M_S.

[a] Here, $\cos\theta^* = \tanh(y^*)$, where $\pm y^*$ is the rapidity of each EM object in the center-of-mass frame and $y^* = \frac{1}{2}(y_1 - y_2)$.

[b] We use a cylindrical coordinate system in which ϕ is the azimuthal angle, r is the radius from the nominal beam line, z points in the proton beam direction, and θ is the polar angle measured with respect to the interaction vertex. The pseudorapidity η is defined as $-\ln(\tan(\theta/2))$. Transverse momentum and energy are the respective projections of momentum measured in the tracking system and energy measured in the calorimeter system onto the $r - \phi$ plane, and are defined as $p_T = p\sin\theta$ and $E_T = E\sin\theta$. Missing E_T ($\not\!\!E_T$) is defined as the magnitude of the vector $-\sum_i E_T^i \hat{n}_i$, where E_T^i is the transverse energy deposited in the i^{th} calorimeter tower for $|\eta| < 3.6$ at CDF and $|\eta| < 4.0$ at DØ. and $\hat{n}_i$ is a unit vector perpendicular to the beam axis and pointing at the i^{th} tower.

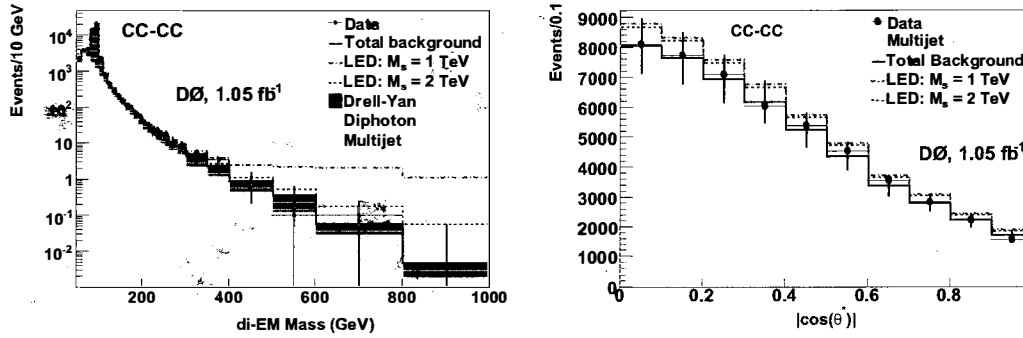

Figure 1: The DØ LED search: the $M_{ee,\gamma\gamma}$ (left) and $|\cos\theta^*|$ (right) distributions, where both EM objects are reconstructed in the central calorimeter. The distributions of the LED signal are obtained by weighting the SM-only full simulation with the ratio of LED+SM to SM parton-level simulations, for $n_d = 4$.

2.2 Search for LED in the Dijet Channel

The DØ Collaboration has also used the shape of $\chi_{\rm dijet}$ [c] distribution to look for LED in the dijet channel in 0.7 fb^{-1} of $p\bar{p}$ collisions [12]. The shape of $\chi_{\rm dijet}$ is flat for Rutherford scattering, and more strongly peaked at small value of $\chi_{\rm dijet}$ in the presence of LED. Using the shape instead of the absolute distribution makes the search less sensitive to the jet energy scale, luminosity, PDF, and renormalization scale. Jets are reconstructed using the midpoint cone algorithm with cone radius of $R = 0.7$.[d] The four-vectors of jets are corrected for the effects of calorimeter response, additional energy from multiple $p\bar{p}$ interactions, shifts in $|y|$ due to detector effects, and bin-to-bin migration due to finite resolutions. Two leading jets are required to have $|y| < 2.4$ each, invariant mass $M_{jj} > 0.25$ TeV/c^2, $\chi_{\rm dijet} < 16$, and $\frac{1}{2}|y_1 + y_2| < 1$. The shapes of the corrected $\chi_{\rm dijet}$ distributions are compared with the SM prediction in bins of M_{jj} from 0.25 TeV/c^2 to above 1.1 TeV/c^2. Since no significant discrepancy is observed between the data and SM prediction, limits on M_S are obtained using the GRW, HLZ, and Hewett formalisms. However, the limits are not as stringent as those from the dielectron and diphoton channels. The same technique is also used to set the world's best limits on the compositeness scales (see Section 3).

2.3 Search for LED in the Mono-photon and Large Missing Energy Channel

The CDF and DØ Collaborations have searched for LED in 2.0 fb^{-1} and 2.7 fb^{-1} of $p\bar{p}$ collisions, respectively, using events with mono-photon and large $\not\!\!E_T$ [13,14]. The analyses require one central photon with $E_T > 90$ GeV and $\not\!\!E_T > 50/70$ GeV for CDF/DØ. Events with extra high p_T tracks or jets are removed. The exclusive $\gamma\not\!\!E_T$ final state suffers from large amount of cosmic rays and beam halos and the analysis would have been impossible if an effective rejection was not applied. The CDF analysis requires the photon to be in time with a $p\bar{p}$ collision and uses topological variables to separate signal from non-collision background, such as track multiplicity, angular separation between the photon and the closest hit in the muon chamber, and energy deposited in the calorimeters. The DØ analysis utilizes the transverse and the unique longitudinal segmentation of the EM calorimeter. The photon trajectory is reconstructed by fitting one measurement in the preshower detector and four in the EM calorimeter to a straight line. The z position and the transverse impact parameter of the photon, at the point of closest approach with respect to the beam line, are required to be within 10 cm and 4 cm of a $p\bar{p}$

[c] Here, $\chi_{\rm dijet} \equiv (1 + \cos\theta^*)/(1 - \cos\theta^*)$.
[d] The R is defined in the y and ϕ plane.

interaction vertex, respectively.[e] The distribution of the transverse impact parameter is further used to estimate the amount of remaining non-collision background. After all selections, the dominant background in both analyses is the SM $Z\gamma \to \nu\nu\gamma$ production. Both analyses have not found significant excess in data: 40 observed vs. 46.3 ± 3.0 expected (CDF) and 51 observed vs. 49.9 ± 4.1 expected (DØ). The lower limits on the fundamental Planck scale, M_D, are obtained at the 95% C.L.: 1080–900 GeV for $n_d = 2 - 6$ from CDF, and 970–804 GeV for $n_d = 2 - 8$ from DØ. The CDF and DØ limits using the $\gamma \not\!\!E_T$ final state supersede the LEP combined limits [15] when $n_d > 3$ and $n_d > 4$, respectively. The CDF Collaboration further combines the mono-photon+$\not\!\!E_T$ and mono-jet+$\not\!\!E_T$ channels and excludes M_D below 1400-940 GeV for $n_d = 2 - 6$.

3 Searches for Quark Compositeness in the Dijet Channel

The proliferation of quarks and leptons suggests that they may be composite structures. The compositeness scale Λ_C characterizes the physical size of composite states. The shapes of $\chi_{\rm dijet}$ distributions in bins of M_{jj} as described in Section 2.2 are also used to set limits on Λ_C, using the matrix elements in Ref. [2]. Data with large M_{jj} are more sensitive to large Λ_C since the deviation from the SM dijet cross section increases as a function of M_{jj}/Λ_C. The best lower limits on Λ_C have been obtained: 2.73 TeV for positive and 2.64 TeV for negative interference between the new physics and the SM.

4 Searches for Leptoquarks in the $\ell\ell jj$ and $\ell \not\!\!E_T jj$ Channels

Leptoquarks (LQs) are predicted in many models to explain the observed symmetry between leptons and quarks, such as technicolor, grand unification theories, superstrings, and quark-lepton compositeness [3]. The DØ Collaboration has looked for pair production of scalar leptoquarks for all three generations in 1.0 fb^{-1} of $p\bar{p}$ collisions, assuming LQs couple to quarks and leptons within the same generation. The $LQ_1LQ_1 \to eejj$ [12], $LQ_2LQ_2 \to \mu\mu jj + \mu \not\!\!E_T jj$ [16], and $LQ_3LQ_3 \to \tau\tau bb$ [17] channels are studied, respectively. The cross section of pair production depends only on mass of LQ, M_{LQ}. The coupling of LQ to charge lepton $\mathcal{B}(LQ \to \ell q)$ is defined as β and the coupling to neutral lepton $\mathcal{B}(LQ \to \nu q)$ is $1 - \beta$. Therefore, the final event rates of $\ell\ell jj$ and $\ell \not\!\!E_T jj$ are proportional to β^2 and $\beta(1-\beta)$. The lepton selections are: (i) $eejj$: $E_T^e > 25$ GeV, $|\eta^e_{1,2}| \; o \; 1.1$ or $|\eta^e_1| \; o \; 1.1$ and $1.5 \; o \; |\eta^e_2| \; o \; 2.5$, (ii) $\mu\mu jj$ and $\mu \not\!\!E_T jj$: $p_T^\mu > 20$ GeV/c, $|\eta^\mu_{1,2}| \; o \; 2.0$, $\not\!\!E_T > 30$ GeV, (iii) $\tau\tau bb$: a hadronic and a leptonic (decaying to μ) τ candidate with $p_T > 15$ GeV/c each, $|\eta_{\rm had}| \; o \; 3.0$, $|\eta_\mu| \; o \; 2.0$. All jets are reconstructed using the midpoint cone algorithm with $R = 0.5$ and required to have $E_T^j > 25$ GeV and $|\eta_{\rm j}| \; o \; 2.5$; the $\tau\tau bb$ analysis requires at least one jet tagged as b-jet. The variable S_T, which is the scalar sum p_T of the two leptons (either $\ell\ell$ or $\ell \not\!\!E_T$), and two highest p_T jets, is then used as a discriminant to set lower limits on M_{LQ}. The lower limits on M_{LQ} assuming fixed values of β are: $M_{LQ_1}^{\beta=1} > 292$ GeV/c^2, $M_{LQ_2}^{\beta=1} > 316$ GeV/c^2, $M_{LQ_2}^{\beta=0.5} > 270$ GeV/c^2, and $M_{LQ_3}^{\beta=1} > 210$ GeV/c^2, $M_{LQ_3}^{\beta=0.5} > 207$ GeV/c^2. For the second generation, the $\mu\mu jj$ and $\mu \not\!\!E_T jj$ final states are also combined to exclude region in the β vs. M_{LQ_2} plane. The cross-talk of $\mu\mu qq$ in the $\mu \not\!\!E_T jj$ events due to the missing muon is taken into account. See Figure 2 for the S_T of $\mu \not\!\!E_T jj$ final state and the exclusion region in the $\beta - M_{LQ_2}$ plane.

[e] The resolution of the z position is ≈ 3 cm and the resolution of the transverse impact parameter is ≈ 2 cm.

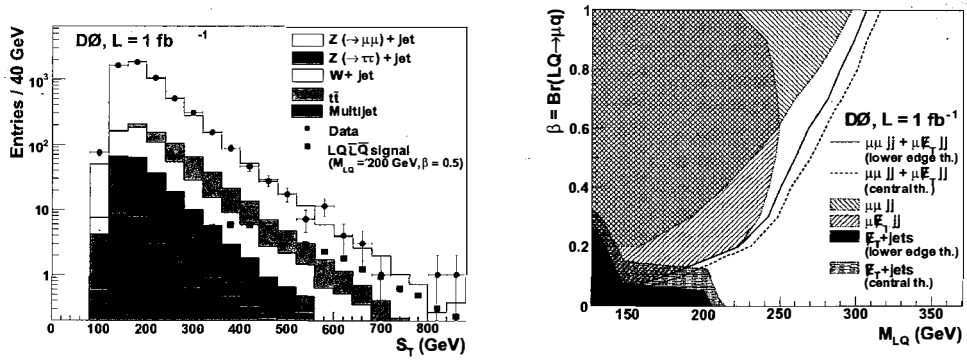

Figure 2: The DØ leptoquark search: the S_T distribution of the $\mu \not\!\!E_T jj$ events (left) and the exclusion region in the β vs. M_{LQ_2} plane (right).

5 Searches for Supersymmetry

Supersymmetry (SUSY) aims to solve the hierarchy problem by introducing superpartners of SM particles [4]. The spin of SUSY particles differs from the original particles by 1/2. For example, the SUSY partners of gluon, graviton, and bottom quark are: gluino ($\tilde{g}$), gravitino ($\tilde{G}$), and sbottom quark ($\tilde{b}$), and carry spin 1/2, 3/2, and 0, respectively. The mixtures of SUSY partners of Z boson (zino), photon (photino), and the neutral Higgs (higgsino) form four mass eigenstates with spin 1/2, and are called neutralinos ($\tilde{\chi}_i^0$; $i = 1 - 4$). In the R-parity conserving SUSY,[f] the lightest SUSY particle (LSP) is stable and will not decay into SM particles, which leaves $\not\!\!E_T$ and provides possible candidates for dark matter. Section 5.1 and Section 5.2 describe the search for SUSY when the LSPs are the lightest neutralino $\tilde{\chi}_1^0$ and gravitino $\tilde{G}$, respectively.

5.1 Search for Gluino-mediated Sbottom Production

In several SUSY models [5], sbottom may be light due to the large mixture between the left- and right-handed sbottom quarks. If $\tilde{b}$ is light enough, it may be produced via the gluino decay: $\tilde{g} \to \tilde{b}b$. For similar mass, the gluino pair-production cross section is an order of magnitude larger than that of sbottom, due to gluino's larger color charge and spin. The CDF Collaboration has searched for production of gluino-mediated sbottom via the decay chain, $\tilde{g}\tilde{g} \to b\bar{b}\tilde{b}\tilde{b}$ and $\tilde{b} \to b\tilde{\chi}_1^0$, which results in a final state with 4 b-jets and large $\not\!\!E_T$. Event selections are at least two jets with $E_T > 25$ GeV (leading jet $E_T > 35$ GeV) and $|\eta| < 2.4$, of which two must be tagged as b-jets by the SECVTX algorithm [18], and $\not\!\!E_T > 70$ GeV. Two types of neural network (NN) are employed to suppress backgrounds from top pair-production and QCD multi-jet events, respectively. The requirements on the NN outputs are optimized for two different regions of $\Delta m \equiv m(\tilde{g}) - m(\tilde{b})$: (i) small Δm, $m(\tilde{g}) = 335$ GeV/c^2 and $m(\tilde{b}) = 315$ GeV/c^2, (ii) large Δm, $m(\tilde{g}) = 335$ GeV/c^2 and $m(\tilde{b}) = 260$ GeV/c^2. After these requirements, 2 (5) events are observed in data, consistent with the background prediction 2.4 ± 0.8 (4.7 ± 1.5) events for small (large) Δm optimization. The excluded region on sbottom mass vs. gluino mass from this analysis shows a significant improvement to the results from previous 156 pb^{-1} analysis and the search for direct pair-production of sbottom (see Figure 3).

[f] R-parity is defined by the spin (j), baryon number (B) and lepton number (L): $R \equiv (-1)^{2j+3B+L}$. By definition, $R = +1$ for SM particles and $R = -1$ for SUSY particles.

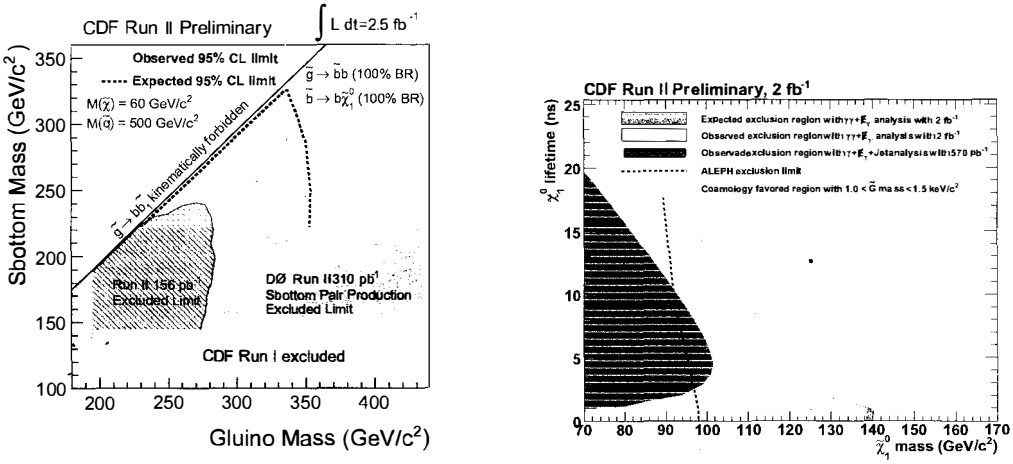

Figure 3: The CDF gluino-mediated sbottom search (left): the exclusion region of sbottom mass vs. gluino mass. The CDF GMSB search (right): the exclusion region of $\widetilde{\chi}_1^0$ lifetime vs. $\widetilde{\chi}_1^0$ mass.

5.2 Search for GMSB in the Diphoton and Large Missing Energy Channel

The CDF Collaboration has searched for gauge-mediated supersymmetry breaking (GMSB)[6] in 2.0 fb^{-1} of $p\bar{p}$ collisions. In GMSB, the next-to-lightest supersymmetry particle $\widetilde{\chi}_1^0$ may decay to the LSP $\widetilde{G}$ (with a mass of a few keV) via $\widetilde{\chi}_1^0 \rightarrow \widetilde{G}\gamma$. Assuming R-parity conservation, pair production of massive SUSY particles, such as $\widetilde{\chi}_2^0\widetilde{\chi}_1^{\pm}$ or $\widetilde{\chi}_1^+\widetilde{\chi}_1^-$, results in a final state with two photons and large $\not\!\!E_T$ due to the escape of the $\widetilde{G}$ from the detector. This analysis considers a minimal GMSB model (Snowmass Slope SPS 8[19]) to quote results as a function of $\widetilde{\chi}_1^0$ mass and lifetime. The requirements are two isolated central photons with $E_T > 13$ GeV each, $\Delta\phi(\gamma_1,\gamma_2) < \pi - 0.15$, $H_T > 200$,[g] and $\not\!\!E_T$ significance > 3. The latter three requirements have been optimized to obtain the best significance of GMSB signal, and also to reduce the background from $W\gamma$ events.[h] In order to calculate the $\not\!\!E_T$ significance, ten pseudo-experiments for each event in data are performed. The $\not\!\!E_T$ significance is defined as $-\log(\mathcal{P})$, where $\mathcal{P}$ is the probability for the $\not\!\!E_T$ drawn from the expected mis-measured $\not\!\!E_T$ distribution[i] to be equal to or larger than the observed $\not\!\!E_T$. Further selections are applied to suppress non-collision background (cosmics, beam halo, photo-tube spikes). After all selections, one event is observed in the data, which is consistent with the background prediction, 0.62 ± 0.29 event. Figure 3 shows the exclusion region in the plane of $\widetilde{\chi}_1^0$ lifetime (up to 2 ns) vs. $\widetilde{\chi}_1^0$ mass. For $\widetilde{\chi}_1^0$ with zero lifetime, the mass below 138 GeV/c^2 is excluded at 95% C.L. These are the best limits to date. Analysis to search for long-lived $\widetilde{\chi}_1^0$ with more than 2 fb^{-1} is work in progress.

6 Conclusion

The CDF and DØ collaborations have a broad program of searching for new physics in photon and jet final states. We have not yet found significant excess in 0.7–2.7 fb^{-1} of $p\bar{p}$ collisions.

[g] The H_T is the scalar sum p_T of all identified objects in the events.

[h] The electron from W is mis-identified as a photon and the two photons are back-to-back due to the large H_T requirement.

[i] The expected mis-measured $\not\!\!E_T$ distribution is modeled by studying: (i) the resolution of unclustered energy with zero-jet events in the $Z \rightarrow ee$ and fake photon data, (ii) the resolution of jet energy with the dijet and Z+jet data.

We have set the best limits to date on parameters predicted by large extra dimension, quark compositeness, leptoquarks, and supersymmetry. As more data data are being collected, we expect many new and interesting results from both CDF and DØ.

Acknowledgments

The author wishes to thank the CDF Exotic and DØ New Phenomena group conveners, M. D'onof T. Wright, T. Adams, and A. Duperrin, for their suggestions which improved this documentation and the presentation in the conference.

References

1. N. Arkani-Hamed, S. Dimopoulos, and G. R. Dvali, *Phys. Lett.* B **429**, 263 (1998).
2. E. Eichten, K. D. Lane, and M. E. Peskin, *Phys. Rev. Lett.* **50**, 811 (1983); P. Chiappetta and M. Perrottet, *Phys. Lett.* B **253**, 489 (1991); K. D. Lane, arXiv:hep-ph/9605257.
3. S. Dimopoulos and L. Susskind, *Nucl. Phys.* B **155**, 237 (1979); J. C. Pati and A. Salam, *Phys. Rev.* D **10**, 275 (1974); H. Georgi and S. L. Glashow, *Phys. Rev. Lett.* **32**, 438 (1974); E. Eichten and K. D. Lane, *Phys. Lett.* B **90**, 125 (1980); B. Schrempp and F. Schrempp, *Phys. Lett.* B **153**, 101 (1985); W. Buchmuller and D. Wyler, *Phys. Lett.* B **177**, 377 (1986); J. L. Hewett and T. G. Rizzo, *Phys. Rept.* **183**, 193 (1989); D. London and J. L. Rosner, *Phys. Rev.* D **34**, 1530 (1986).
4. S. P. Martin, arXiv:hep-ph/9709356.
5. A. Bartl, W. Majerotto, and W. Porod, *Z. Phys.* C **64**, 499 (1994) [Erratum-ibid. C **68**, 518 (1995)]; W. Beenakker, R. Hopker, M. Spira, and P. M. Zerwas, *Nucl. Phys.* B **492**, 51 (1997).
6. S. Ambrosanio, G. L. Kane, G. D. Kribs, S. P. Martin, and S. Mrenna, *Phys. Rev.* D **54**, 5395 (1996); C. H. Chen and J. F. Gunion, *Phys. Rev.* D **58**, 075005 (1998).
7. G. F. Giudice, R. Rattazzi, and J. D. Wells, *Nucl. Phys.* B **544**, 3 (1999).
8. T. Han, J. D. Lykken, and R. J. Zhang, *Phys. Rev.* D **59**, 105006 (1999).
9. J. L. Hewett, *Phys. Rev. Lett.* **82**, 4765 (1999).
10. V. M. Abazov *et al.* (DØ Collaboration), *Phys. Rev. Lett.* **102**, 051601 (2009).
11. T. Sjöstrand, S. Mrenna, and P. Skands, *J. High Energy Phys.* **05**, 026 (2006).
12. J. F. Grivaz, *Int. J. Mod. Phys.* A **23**, 3849 (2008).
13. T. Aaltonen *et al.* (CDF Collaboration), *Phys. Rev. Lett.* **101**, 181602 (2008).
14. E. Carrera (DØ Collaboration), arXiv:0810.1331 [hep-ex].
15. C. Amsler *et al.* (Particle Data Group), *Phys. Lett.* B **667**, 1 (2008).
16. V. M. Abazov *et al.* (DØ Collaboration), *Phys. Lett.* B **671**, 224 (2009).
17. V. M. Abazov *et al.* (DØ Collaboration), *Phys. Rev. Lett.* **101**, 241802 (2008).
18. D. Acosta *et al.* (CDF Collaboration), *Phys. Rev.* D **71**, 052003 (2005); C. Neu, FERMILAB-CONF-06-162-E (2006).
19. B. C. Allanach *et al.*, *Eur. Phys. J.* C**25**, 113 (2002).